Polar catastrophe and the structure of KTa_{1−x}Nb_{x}O_{3} surfaces: Results from elastic and inelastic helium atom scattering

F. A. Flaherty, T. W. Trelenberg, J. A. Li, R. Fatema, J. G. Skofronick, D. H. Van Winkle, S. A. Safron, and L. A. Boatner

Phys. Rev. B **92**, 035414 — Published 13 July 2015

DOI: 10.1103/PhysRevB.92.035414

Polar Catastrophe and the Structure of KTN Surfaces: Results from Elastic and Inelastic Helium Atom Scattering

Francis A. Flaherty*
Department of Physics, Valdosta State University, Valdosta, GA 31698-0055

T. W. Trelenberg, Jaime A. Li, Rifat Fatema†, J. G. Skofronick, David H. Van Winkle‡
Department of Physics, Florida State University, Tallahassee, FL 32306-4350

Sanford A. Safron
Department of Chemistry and Biochemistry, Florida State University, Tallahassee, FL 32306-4390

L. A. Boatner
Oak Ridge National Laboratory, Oak Ridge, TN 37831

The structure and dynamics of cleaved (001) surfaces of potassium tantalates doped with niobium, $KTa_{1-x}Nb_xO_3$ (KTN) with x ranging from 0 to 30%, were measured by helium atom scattering (HAS). Through HAS time-of-flight (TOF) experiments, a dispersionless branch (Einstein phonon branch) with energy of 13 to 14 meV was observed across the surface Brillouin zone in all samples. When this observation is combined with the results from earlier experimental and theoretical studies on these materials, a consistent picture of the stable surface structure emerges: After cleaving the single crystal sample, the surface should be composed of equal areas of KO and TaO_2/NbO_2 terraces. The data, however, suggest that K^+ and O^{2-} ions migrate from the bulk to the surface forming a charged KO lattice that is neutralized primarily by additional K^+ ions bridging pairs of surface oxygens. This structural and dynamic modification at the (001) surface of KTN appears due to its formally charged KO(-1) and TaO_2/NbO_2(+1) layers and avoids a "polar catastrophe". This behavior is contrasted with the (001) surface behavior of the fluoride perovskite $KMnF_3$ with its electrically neutral KF and MnF_2 layers.

PACS numbers 68.35.B-, 68.35.Ja, 68.47.Gh, 68.49.Bc
Keywords: Helium Atom Scattering, Polar Catastrophe, Perovskite Surface Structure, Surface Phonon, Einstein Phonon Branch

As a class of materials, perovskites have long been associated with characteristic phase transformations and behaviors in which they often exhibit technologically useful effects, such as ferroelectricity and piezoelectricity[1,2], and show potential in solar cells[3,4] and as photovoltaic materials.[5] The helium atom scattering (HAS) laboratory group at FSU has investigated cleaved (001) perovskite surfaces, particularly potassium tantalate ($KTaO_3$)[6], and potassium tantalate doped with Nb (KTN)[7-9] or lithium (KLT).[9,10] When cleaved, the fresh surfaces are nominally composed of layers, KO/LiO and TaO_2/NbO_2, that are formally charged -1 and +1, respectively. A crystal structure composed of alternating equally but oppositely charged layers, such as KO and TaO_2, would result in an unbounded increase in electrical potential at the surface, termed a "polar catastrophe".[11]. Charge redistribution is necessary to prevent this. In this paper we present evidence that ion migration from the bulk to the freshly cleaved surface is the mechanism for this redistribution for several different KTN crystals. This behavior should be compared with the charge redistribution mechanism proposed to avoid the polar catastrophe in lanthanum aluminate ($LaAlO_3$) layers grown on strontium titanate

($SrTiO_3$).[11-14] Our results contrast with those from similar HAS experiments on the fluoride perovskite $KMnF_3$.[15]

In recent work studying the (100) interface of $LaAlO_3$ and strontium titanate $SrTiO_3$, researchers have found unexpected electrical conduction, magnetism and superconductivity.[11-14,16-25] The perovskite structure of $LaAlO_3$ consists of (100) LaO and AlO_2 layers, which are formally charged +1 and -1, respectively. The corresponding (100) layers of $SrTiO_3$, SrO and TiO_2 are formally electrically neutral. When $LaAlO_3$ is grown on a $SrTiO_3$ substrate, beginning with an LaO layer on a TiO_2 layer, a "conducting electron gas" forms at the interface after four or more layers of $LaAlO_3$ are deposited.[12] This is understood as being associated with the charge redistribution needed to "avoid" the polar catastrophe that would arise from the deposition of many alternating charged LaO and AlO_2 layers. Proposed mechanisms for producing this conducting gas include the formation of oxygen vacancies in the deposition process[23-25], polar distortions[20-22] and metal ion intermixing at the interface.[17] Metal ion intermixing was found to alleviate polarity conflict at the $KTaO_3/GdScO_3$ perovskite interface[26] However, the roles played by these factors in leading to the observed interfacial behavior for $LaAlO_3/SrTiO_3$ are still under investigation. Experiments employing angle resolved photoelectron spectroscopy (ARPES) on targets of $SrTiO_3$ produced by cleaving at very low temperatures (10-20 K) have found evidence for a two-dimensional electron gas in the near-surface region.[27] Although the termination of the surface was not determined in these studies, this result is ascribed to the presence at the surface of oxygen vacancies. These arise from doping of the $SrTiO_3$ crystals prior to cleaving and from the cleaving process itself at these temperatures.[27]

The FSU HAS laboratory has employed low-energy helium atom scattering to investigate the structure of (001) surfaces of potassium tantalate doped to various levels with niobium, $KTa_{1-x}Nb_xO_3$ (KTN), with x ranging from 0 to 30%, through angular distributions (ADs) and drift spectra (DS) experiments.[4-7] The experimental techniques have been described in detail in previous articles from this laboratory.[6,7] Briefly, ADs are measurements of the intensity of the elastically scattered He atoms as a function of scattering angle. They reveal diffractive interference in the atom scattering due to the periodic surface structure. This effect gives rise to Bragg diffraction peaks that characterize the surface and from which the surface lattice parameters can be determined. Interference also affects the intensity of He atoms scattered to the same angle from surface terraces separated by spacings normal to the surface. In this case, it manifests as oscillations in the intensities of diffraction peaks as the He wave vector (wavelength) is varied. DS experiments are measurements of these intensity oscillations for the specular diffraction peak. The Fourier transform of a DS yields the distribution of step heights among the surface terraces for that surface.[28]

As both AD and DS measurements rely on the coherent scattering of the He atoms, they are particularly sensitive to surface disorder due to random adsorbates and defects. Hence, the experiments were carried out under ultra-high vacuum (UHV, $< 10^{-9}$ mbar) conditions. Further, each KTN target was prepared by cleaving a single-crystal sample of the KTN *in situ* and kept at relatively low temperatures ($\leq$300 K). (See Figure 1a for a typical AD.) Statistically, cleaving a sample of a KTN should produce a (001) target whose surface area is 50% KO and 50% TaO_2/NbO_2. As noted above, these layers are formally charged, -1 for KO and +1 for TaO_2/NbO_2. Since the unit cell dimensions for KTNs are all nearly the same, about 3.98 Å[29], step heights between KO terraces and TaO_2/NbO_2 terraces should measure approximately 2 Å + n(4 Å), where n is an integer.

However, this is not what was observed. First, ADs of He diffraction measured in the region around the specular angle soon after cleaving showed peaks or broadened shoulders flanking the specular diffraction peak.[30,6,7,10] These gradually disappeared in measurements repeated over a period of about an hour until a single, sharp specular peak remained. At this point, the peaks in the diffraction pattern from the surface appeared sharp and stable. These measurements demonstrated that initially the cleaved surface, with its charged KO and TaO_2/NbO_2 terraces, is not stable.

Second, after the surface of a target stabilized, several different experiments could be performed. Among these were DS to determine the step-height distribution of terraces at the surface. In all cases for targets with Nb doping levels up to 20%, the Fourier transform of the oscillations in the specular peak intensities revealed that the principal step height between terraces was 4 Å.[7-10] A step height of 8 Å was also seen in almost all experiments, but with a much smaller probability. A step height of 6 Å with even lower probability was found in only a few experiments. These measurements showed that the modifications occurring after cleaving almost always eliminate the 2 Å step height separation expected between the KO and TaO_2/NbO_2 terraces.

Several perovskite (ABO_3) surfaces were studied by Szot et al. using x-rays.[31] Their experiments showed that at high temperatures (500-1000°C) the surfaces of their powdered materials consist of AO complexes or compounds of the form $AO^*(ABO_3)_n$. These arise as the result of migration of A and O ions from the bulk to the surface. In the case of $KTaO_3$, they also studied the surface with secondary ion mass spectrometry (SIMS) and atomic force microscopy (AFM).[29] The AFM technique showed marked changes in the surface morphology after heating to 700°C. SIMS performed after heat treatment showed "...enrichment of K relative to Ta close to the surface and a corresponding depletion in deeper parts of the near surface region."

Unlike the high temperature experiments of Szot *et al.*, the HAS experiments reported by the FSU lab were all carried out with target temperatures at or below room temperature. Despite this significant temperature difference, the results of the atom diffraction experiments are consistent with the migration of K^+ and O^{2-} ions to the surface from the near-surface bulk. Furthermore, the near-absence of 2 Å step heights in the analyses of the drift spectra and the predominance of step heights with the unit cell dimension of 4 Å suggest that these migrating ions predominantly cover the TaO_2/NbO_2 regions of the cleaved surface with a KO lattice.

Fritsch and Schröder performed theoretical calculations for the charged KO surface of $KTaO_3$.[6,34] They found, first, that electron transfer occurs from surface oxygens to sub-surface tantalums so that the average formal charge of a surface KO is reduced from -1 to -½. They also obtained a slight relaxation of the surface oxygens that leads to additional stabilization. Further calculations[6] showed that extra K^+ ions can be stably bound to the surface oxygens, with the most stable arrangement having a K^+ ion bound between two oxygens as a bridge in a <10> or <01> direction. The calculated normal vibrational frequency of this ion corresponds to a phonon mode with energy of 12.8meV.

We note that recent global optimization calculations have suggested a somewhat different structure for the stable (001) surface of $KTaO_3$. While these also require ion migration from the near-surface region, they additionally involve cation exchanges.[33]

AD experiments in the FSU HAS laboratory on cleaved, single-crystal KTN targets, in both <10> and <11> high symmetry azimuths, yielded Bragg peaks consistent with the 4 Å surface lattice parameter expected for both KO and TaO_2/NbO_2 layers.[4-7] (See Figure 1a.) Hence, the KO surface formed after stabilization appears essentially the same as the KO layer produced by the cleaving. Additionally, it was found that He atom diffraction from cleaved

targets which were cooled to temperatures less than 100 K and then warmed above180 K showed small, broad half-order diffraction peaks in addition to the large, sharp integer-order peaks. These peaks were found only in ADs carried out in the <10> azimuth; they were never observed in ADs in the <11> azimuth. These results indicate that small (2×1) domains, typically with dimensions of about 50 Å, as determined from the widths of the half-order peaks, had formed on at least part of the surface as the result of thermally cycling to low temperatures.[6-8] The half-order peaks disappeared from the diffraction pattern when the target was warmed above 330K.[6]

In similar HAS diffraction experiments on the fluoride perovskite $KMnF_3$[15], Toennies and Vollmer observed much longer-lived metastable peaks flanking the specular peak. These diminished in about 20 days rather than in about an hour as found for the KTNs. $KMnF_3$ also yields two (100) layers upon cleaving, KF and MnF_2, but these layers are not formally charged. The long lifetimes of the metastable peaks were attributed to the merging of small KF and MnF_2 terraces formed in the cleaving to produce more stable larger ones. DS carried out on this material yielded step heights of about 2 Å that indicated the coexistence of terraces of these two layers in the stable (001) surface. These studies also revealed half-order diffraction peaks in AD measurements below 191 K. However, they appeared in both high symmetry azimuths, corresponding to a (2×2) structure, and were found to be associated with a bulk phase transition at 187.5 K. In contrast, the temperatures of appearance of the KTN (2×1) domains, noted above, were very similar for all KTNs despite the great variation of ferroelectric transition temperatures as a function of Nb concentration. Pure $KTaO_3$, in fact, is an incipient ferroelectric and has no solid bulk phase transition. Thus, we conclude that the appearance of (2×1) domains in KTN is not associated with any bulk phase transition.

Two obvious factors contribute to these differences between the behaviors of KTN and $KMnF_3$. One is the difference in the chemistries of O^{2-} *vs* F^- ions. The second is the surface electrostatics. The KO and TaO_2/NbO_2 layers are formally charged, whereas the KF and MnF_2 layers are neutral.

Measurements of surface phonon energies of the KTN materials were carried out in the FSU laboratory by means of time-of-flight (TOF) inelastic HAS investigations.[6-9] These data were all obtained on the same sample that was cleaved at a chamber pressure of 2x10-10 Torr over a period of 6 days. The sample temperature was raised to 300K for 5 minutes before each measurement in order to minimize surface. For every target tested, including those displaying half-order diffraction peaks, the greatest intensities obtained in TOF spectra in both high symmetry directions and across the surface Brillouin zone (SBZ) correspond to phonon modes forming an Einstein branch. The energies of this branch vary slightly, but range from 13 to 14 meV. The essentially dispersionless character of the branch and the vibrational energies that are virtually the same as those calculated by Fritsch and Schröder suggest that the stable surface comprises K^+ ions bridging surface oxygens on a KO lattice and acting as nearly-independent oscillators.

The results of TOF HAS experiments on a target with 20% Nb doping provide the strongest evidence for the existence of these oscillators. This sample cleaved poorly. The resulting target gave weak and very broad diffraction peaks in ADs, and a large diffuse scattering background. (See Figure 1b.) The peak widths yielded an estimated terrace dimension of approximately 30 Å as compared to a more typical AD shown in Figure 1a, where the estimated terrace dimensions are about 10 times greater.

Nevertheless, the TOF experiments on this 20% Nb target still produced strong inelastic scattering peaks in TOF spectra that correspond to surface phonons with energies in the range of

13 to 14 meV. Figure 2a shows a typical TOF spectrum, converted to energy transfer, for a 20% Nb-doped sample. Figure 3 shows the phonon energies for this mode across the SBZ in the <10> azimuth for three target temperatures. The surface was prepared by cleaving at 190K under UHV conditions, and then aligned to give the best He angular distribution possible for this surface. Additional angular distributions were measured at several temperatures ranging from 240K to 140K. The TOF measurements were carried out during a period of 10 days from the cleaving, first at 190K, then at 240K and then at 140K. For the measurements at 140K, the surface was flashed to 300K after every three TOF spectra were recorded to minimize any surface contamination. The fits give an average energy of 13.4 ± 0.4 meV. Targets with very good surface quality, as indicated by sharp diffraction peaks in their ADs such as the one shown in Figure 1a, often yield inelastic scattering peaks in their TOF spectra in addition to those corresponding to this Einstein phonon branch. These TOF peaks almost always turn out to be due to phonon modes with energies somewhat lower than 13 meV. An example, for comparison, is presented in Figure 2b. Unlike the phonons of the Einstein branch, the energies of these phonons usually show temperature dependent dispersion. For the 20% Nb targets, however, no other vibrational modes were ever observed.

We note that the wavelengths of the phonons towards the SBZ center in this dispersionless branch are much larger than the approximately 30 Å terrace dimension. This strongly supports the suggestion that these inelastic TOF peaks arise from isolated oscillators, consistent with the picture of bridging K^+ ions at the surface. That is, despite the poor quality of the surface, this target still appears to have many independent oscillators with essentially the energy calculated by Fritsch and Schröder.[34]

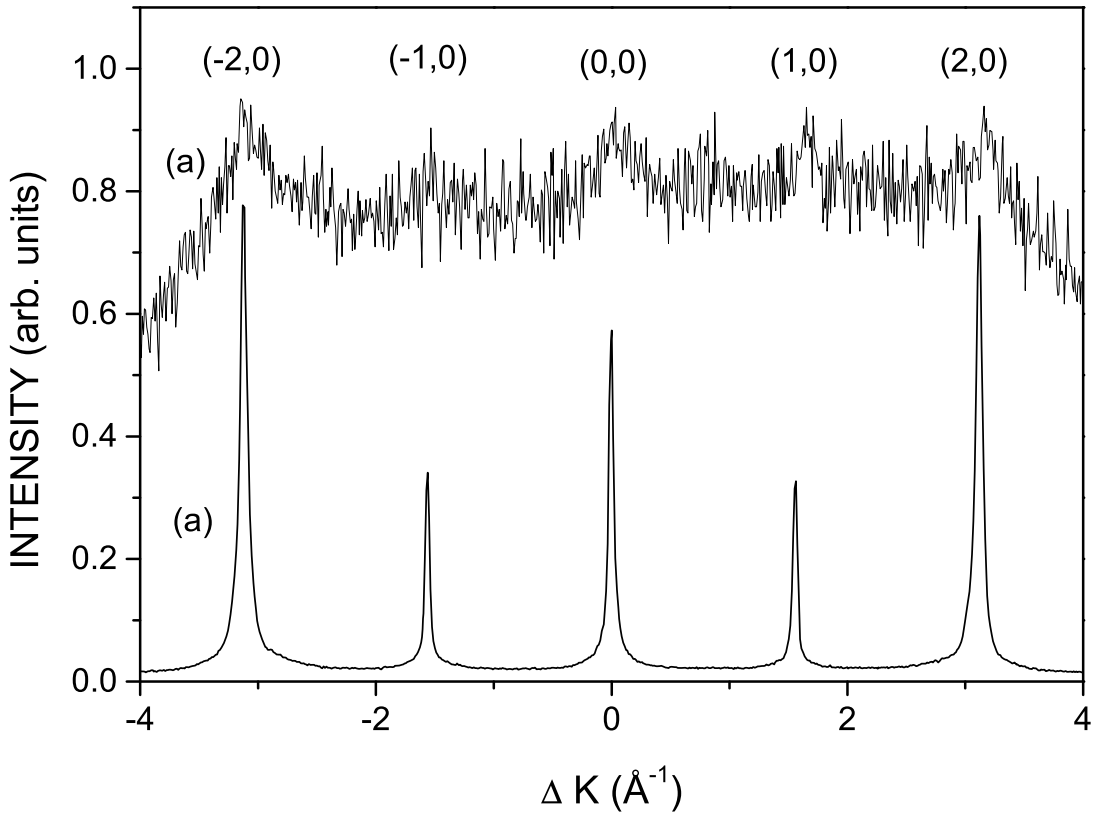

FIG. 1: HAS angular distribution measurements in the <10> azimuth are shown, with angle converted to parallel momentum transfer ΔK, for the cleaved (001) surfaces of (a) 10% Nb-doped KTN and (b) 20% Nb-doped KTN. For both, the incident wave vector $k_i = 7.88$ Å^{-1} and the target temperature is 190 K. The ordinate scales are arbitrary and have been displaced for clarity.

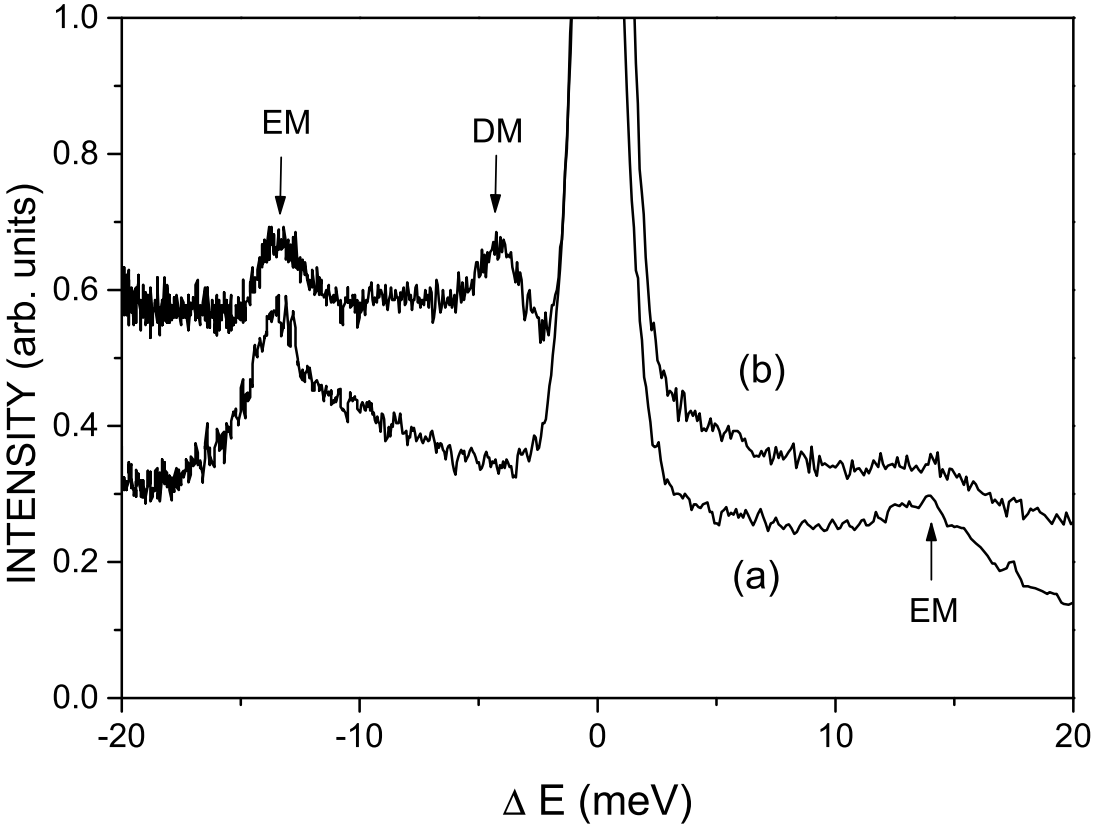
1.0
0.8
0.6
0.4
0.2
0.0
INTENSITY (arb. units)
EM
DM
(b)
(a)
EM
-20
-10
0
10
20
Δ E (meV)

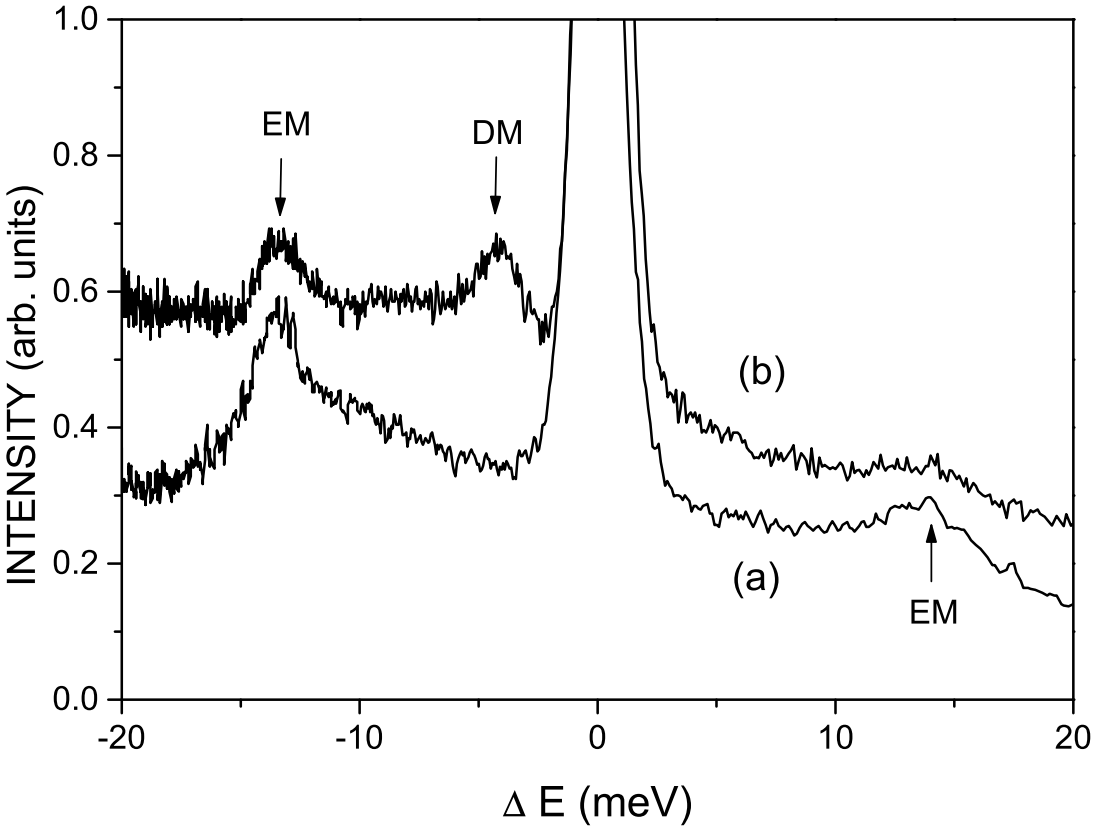

FIG. 2: HAS TOF measurements in the <10> azimuth with $k_i = 7.88$ Å^{-1}, converted to energy transfer ΔE, for the cleaved (001) surfaces of (a) 20% Nb-doped KTN at target temperature 190 K and scattering angle 58° and (b) pure potassium tantalate at target temperature 220 K and scattering angle 58.5°. The positions indicated by EM correspond to energy transfers for the Einstein phonon modes; the position labeled DM corresponds to energy transfer of a phonon in a dispersive branch. The ordinate scales are arbitrary and have been displaced for clarity.

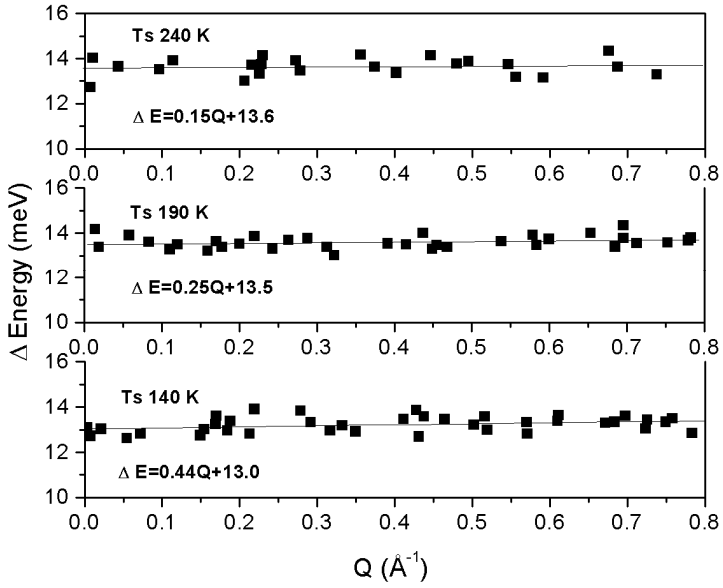

FIG. 3: Surface phonon dispersion curves in the <10> azimuth for the cleaved (001) surface of 20% Nb-doped KTN at target temperatures of 140K, 190K, and 240K, obtained by folding the TOF energy transfer measurements into the first surface Brillouin zone. The solid lines are the best-fit straight lines through the data points, with the fit equations shown for each data set. The standard deviation is approximately 0.4 meV. The lattice parameter *a* is 3.98 Å; the SBZ boundary is 0.79 $Å^{-1}$.

The TOF HAS experiments on $KMnF_3$ again provide a strong contrast to the KTN results.[13] Significantly, for $KMnF_3$ no Einstein phonon branch was observed in either high symmetry azimuth. Surface phonon branches typically follow the bulk phonon band edges in the corresponding bulk Brillouin zone. The dispersion curves for $KMnF_3$ measured in the two high symmetry directions differ from each other, as expected, since the bulk dispersion curves corresponding to these surface azimuths differ.[15]

We briefly summarize the HAS experimental results on the KTNs. (1) Repeated He diffraction measurements near the specular reflection peak soon after cleaving KTN samples showed metastable behavior. (2) Analyses of drift spectra obtained from stable KTN surfaces (with Nb ≤20%) yielded a principal step-height between terraces of 4 Å rather than the 2 Å expected from the perovskite structure. (3) TOF HAS revealed a dispersionless phonon branch in the energy range of 13 to 14 meV. (4) Small and broad half-order diffraction peaks were observed in He diffraction of targets cooled below 100 K only in the <10> high symmetry azimuth; the peaks disappeared when the targets were warmed above 330 K.

These HAS results, combined with the theoretical calculations, suggest that (1) K^+ and O^{2-} ions migrate from the bulk to the surface after cleaving, consistent with the experiments of Szot *et al.*[31,32], to form KO surface terraces. (2) K^+ ions bridging pairs of surface oxygens act as independent oscillators, in agreement with calculations by Fritsch and Schröder.[6,34] (3) The bridging K^+ ions, initially randomly arranged on the KO surface, order into (2×1) and (1×2) domains when the target is thermally cycled to low temperatures, and become disordered again

when the target is warmed above 330 K. A schematic illustration of the surface is presented in Figure 4.

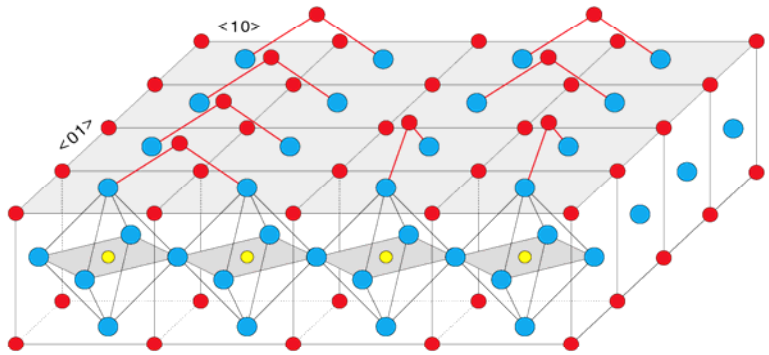

FIG. 4: A schematic representation of the (001) surface of the KTN crystal after reconstruction. The large circles represent O^{2-} ions, the mid-sized circles the K^{+} ions and the smallest circles the Ta/Nb ions. Note that in this schematic six of the bridging K^{+} ions are oriented in the <10> direction; two are oriented in the <01> direction. The K^{+} depicted above the top shadowed surface bridge pairs of O^{2-} ions. It is the vibration of these bridging K^{+} ions that are responsible for the Einstein branch. Note also that the bridging ions impose a local 2x1 symmetry.

The KTN (001) surfaces examined in this laboratory contrast sharply with those of $KMnF_3$ studied by similar HAS experiments[15]. This is likely due to the charged KO and TaO_2/NbO_2 layers in the KTNs *vs* the neutral KF and MnF_2 layers in $KMnF_3$ that are exposed when the respective samples are cleaved. However, the differences must also be influenced by the much smaller size and polarizability of F^{-} compared to O^{2-} that lead to tighter bonding to the metal ions and fewer vacancies, and to the ability of a surface O^{2-} to transfer an electron to an acceptor in the bulk.

A simple calculation shows that a structure consisting of alternating charged +1 and -1 layers must result in an unbounded electrical potential, a polar catastrophe. The helium atom scattering AD, DS and TOF measurements in the FSU laboratory, together with theoretical calculations, show how the KTN (001) surface "avoids" a polar catastrophe. Whereas a cleaved (001) surface of KTN is nominally expected to be 50% KO and 50% TaO_2/NbO_2, the experiments show that K^{+} and O^{2-} ions migrate from the near-surface bulk to form a nearly complete KO surface. Calculations suggest that this charged surface is neutralized by additional K^{+} ions that bridge pairs of surface oxygens. The experiments show a dispersionless phonon branch with energy predicted for these K^{+} ions. The experiments further suggest that these ions, initially randomly ordered, form ordered domains at low temperature and become disordered again when the temperature is raised.

It should be emphasized that the results presented here for the avoidance of a polar catastrophe for cleaved KTN surfaces represents a model system. The surfaces are prepared in a

pristine environment and examined by very surface-sensitive techniques. The experimental results are illuminated by careful theoretical modeling.

Acknowledgement

The authors wish to acknowledge the U. S. Department of Energy for partial support of this research through Grant No. DE-FG02-97ER45635. Research at the Oak Ridge National Laboratory for one author (LAB) was sponsored by the U. S. Department of Energy, Basic Energy Sciences, Material Sciences and Engineering Division. Data analysis by one author (FAF) was facilitated by a Faculty Research Seed Grant from Valdosta State University. The authors wish to thank Scott Baxter for rendering Figure 4.

References

*Electronic address: flaherty@valdosta.edu

† Present address Florida State University-Panama City campus, FL 32405; Gulf Coast State College, Panama City, FL 32401.

‡Electronic address: rip@phy.fsu.edu

1. B. A. Strukov and A. P. Levanyuk, *Ferroelectric Phenomena in Crystals*, (Springer, Berlin, 1998).

2. M. Lines and A. M. Glass, *Principles and Applications of Ferroelectrics and Related Materials* (Clarendon, Oxford, 1977).

3. T. Hamann, Science **345**, 1566-1567 (2014).

4. H. J. Snaith, J. Phys. Chem. Lett. **4**, 3623-3630 (2013).

5. I. Grinberg, D. V. West, M. Torres, G. Gou, D. M. Stein, L. Wu, G. Chen, E. M. Gallo, A. R. Akbashev, P. K. Davies, J. E. Spanier and A. M. Rappe, Nature **503**, 509-512 (2013).

6. J. A. Li, E. A. Akhadov, J. Baker, L. A. Boatner, D. Bonart, J. Fritsch, S. A. Safron, U. Schröder, J. G. Skofronick and T. W. Trelenberg, Phys. Rev. B **68**, 045402 (2003).

7. T. W.Trelenberg, R. Fatema, J. A. Li, E. A. Akhadov, D. H. Van Winkle, J. G. Skofronick, S. A. Safron, F. A. Flaherty and L. A. Boatner, J. Phys.: Condens. Matter **22,** 304009 (2010).

8. R. Fatema, T. W. Trelenberg, D. H. Van Winkle, J. G. Skofronick, S. A. Safron, F. A. Flaherty and L. A. Boatner, Phys. Rev. B **84** 144114 (2011).

9. R. Fatema, Ph.D. Dissertation, Florida State University, (2009), http://diginole.lib.fsu.edu//etd/4495/.

10. R. Fatema, D. H. Van Winkle, J. G. Skofronick, S. A. Safron, F. A. Flaherty and L. A. Boatner, Phys. Rev. B **87**, 085419 (2013).

11. N. Nakagawa, H. Y. Hwang and D. A. Muller, Nature Materials, **5**, 204-209 (2006).

12. P. Zubko, S. Gariglio, M. Gabay, P. Ghosez and J.-M. Triscone, Annu. Rev. Condens. Matter Phys. (2011), 2:141-65.

13. H. Y. Hwang, Y. Iwasa, M. Kawasaki, R. Keimer, N. Nagaosa and Y. Tokura, Nature Materials **11,** 103-113 (2012).

14. H. Hilgenkamp, MRS Bulletin **38**, 1026-1031 (2013).

15. J. P. Toennies and R. Vollmer, Phys. Rev. B **44**, 9833-9852 (1991).

16. C. W. Schneider, S. Thiel, G. Hammerl, C. Richter and J. Mannhart, Appl. Phys. Lett. **89**, 122101 (2006).

17. P. R. Willmott, S. A. Pauli, R. Herger, C. M. Schlepütz, D. Martoccia, B. D. Patterson, B. Delley, R. Clarke, D. Kumah, C. Cionca and Y. Yacoby, Phys. Rev. Lett. **99**, 155502 (2007).

18. C. Cen, S. Thiel, G. Hammerl, C. W. Schneider, K. E. Andersen, C. S. Helberg, J. Mannhart and J. Levy, Nature Mater. **7**, 298-302 (2008).

19. P. Moetakef, T. A. Cain, D. G. Ouellette, J. Y. Zhang, D. O. Klenov, A. Janotti, C. G. Van de Walle, S. Rajan, S. J. Allen and S. Stemmer, Appl. Phys. Lett. **99**, 232116 (2011).
20. R. Pentcheva and W. E. Pickett, Phys. Rev. Lett. **102**, 107602 (2009).
21. S. Savoia, D. Paparo, P. Perna, Z. Ristic, M. Salluzzo, F. Miletto Granozio, U. Scotti di Uccio, C. Richter, S. Thiel, J. Mannhart and L. Marrucci, Phys. Rev. B **80**, 075110 (2009).
22. S. A. Pauli, S. J. Leake, B. Delley, M. Björek, C. W. Schneider, C. M. Schlepütz, D. Martoccia, S. Paetel, J. Mannhart and P. R. Willmott, Phys. Rev. Lett. **106**, 036101 (2011).
23. A. Kalabukhov, R. Gunnarsson, T. Claeson and D. Winkler, http://arxiv.org/abs/cond-mat/0704.1050.
24. C. Li, Q. Xu, Z. Wen, S. Zhang, A. Li and D. Wu, Appl. Phys. Lett. **103**, 201602 (2013).
25. For a recent discussion, see Z. Q. Liu, C. J. Li, W. M. Lü, X. H. Huang, Z. Huang, S. W. Zeng, X. P. Qiu, L. S. Huang, A. Annadi, J. S. Chen, J. M. D. Coey, T. Venkatesan and Ariando, Phys. Rev. X **3**, 021010 (2013).
26. J. Thompson, J. Hwang, J. Nichols, J. G. Connell, S. Stemmer and S. S. A. Seo, Appl. Phys. Lett. **105**, 102901 (2014).
27. A. F. Santander-Syro, O. Copie, T. Kondo, F. Fortuna, S. Pailhès, R. Weht, X. G. Qiu, F. Bertran, A. Nicolaou, A. Taleb-Ibrahimi, P. Le Fèvre, G. Herranz, M. Bibes, N. Reyren, Y. Apertet, P. Lecoeur, A. Barthélémy and M. J. Rozenberg, Nature **469**, 189-193 (2011).
28. D. A. Hamburger, A. T. Yinnon, I. Farbman, A. Ben-Shaul and R. B. Gerber, Surf. Sci. **327**, 165-191 (1995).
29. R. W. G. Wyckoff, *Crystal Structures* (Interscience, New York, 1963) Vol. 2.
30. J. A. Li, E. A. Akhadov, J. Baker, L. A. Boatner, D. Bonart, F. A. Flaherty, J. Fritsch, S. A. Safron, U. Schröder, J. G. Skofronick, T. W. Trelenberg, D. H. Van Winkle, Phys. Rev. Lett. **86**, 4867-4870 (2001).
31. K. Szot, M. Pawelczyk, J. Herion, Ch. Freiburg, J. Albers, R. Waser, J. Hulliger, J. Kwapulinski and J. Dee, Appl. Phys. A **62**, 335-343 (1996).
32. K. Szot, W. Speier, M. Pawelczyk, J. Kwapulinski, J. Hulliger, H. Hesse, U. Breuer and W. Quadakkers, J. Phys.: Condens. Matter **12**, 4687-4697 (2000).
33. D. E. E. Deacon-Smith, D. O. Scanlon, C. R. A. Catlow, A. A. Sokol and S. M. Woodley, Adv. Mater. DOI: 10.1002/adma.201401858 (2014).
34. J. Fritsch and U. Schröder, Phys. Stat. Sol. **215**, 827-831 (1999).